Inorganic Chemistry

Article

pubs.acs.org/IC

Pressure-Dependent Increase in T_c and Magnetic Behavior of $[Ru_2(O_2CBu^t)_4]_3[M(CN)_6]\cdot 2H_2O$ (M = Cr, Fe)

Jack G. DaSilva and Joel S. Miller*

Department of Chemistry, 315 S 1400 East, University of Utah, Salt Lake City, Utah 84112-0850, United States

ABSTRACT: Magnetization as a function of applied pressure up to 10.16 kbar and magnetic field were obtained for layered $[Ru_2(O_2CBu^t)_4]_3[M(CN)_6]\cdot 2H_2O$ (M = Cr, Fe). For M = Fe, the T_c increased by 13% from 6.1 to 6.9 K with a significant increase in the coercive field, H_{cr}, from 5 to 65 Oe, followed by a sharp decrease to less than 10 Oe at further applied pressure. A 32% increase in T_c from 37.8 to 50.0 K was observed for M = Cr as well as a linear decrease of H_{cr} upon increasing pressure from 6380 to 2380 Oe.

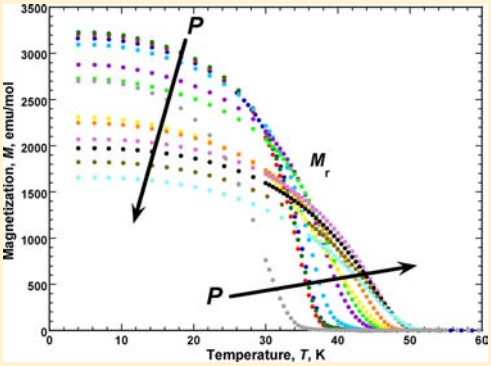

INTRODUCTION

The production excluding utilization of magnets is expected to reach $17.2 billion worldwide by 2020.[1] This has focused research toward the discovery, comprehension, and development of cheaper, more efficient, and stronger magnets that have quantum characteristics coupled to their magnetic behavior. The discovery of the first ferromagnetic organic-based magnet,[2−5] $[Fe^{III}Cp^*_2][TCNE]$ (TCNE = tetracyanoethylene; Cp* = pentmethylcyclopentadienide),[6,7] led to promising routes to photomagnetic,[8] optoelectronic,[9] and magnetoelectric materials.[9] While $[FeCp^*_2][TCNE]$ orders magnetically at 4.8 K,[6,7] other organic-based magnets have higher critical temperatures (T_c), with some extending to room temperature, e.g., $V(TCNE)_x$ ($x \sim 2$; $T_c \sim 127$ °C, 400 K)[10,11] and $V_x[Cr^{III}(CN)_6]$ ($T_c \sim 100$ °C, 373 K).[12−14]

Among the growing number of organic-based magnets is a family of compounds based upon diruthenium acetate paddlewheel (D_{4h}) structured materials. Most notably, diruthenium acetate $[Ru_2(O_2CMe)_4]^+$ when reacted with $[Cr(CN)_6]^{3-}$ forms $[Ru_2(O_2CMe)_4]_3[Cr(CN)_6]$, **1**, that possesses two interpenetrating sublattices that each have alternating $S = {}^3/_2$ $[Ru_2(O_2CMe)_4]^+$ and $S = {}^3/_2$ $[Cr(CN)_6]^{3-}$ ions.[15,16]Compound **1** exhibits an unusual pressure-dependent magnetic behavior including a transition from a metamagnetic-like phase to a ferromagnetic-like phase with an 83% increase in T_c.[17] This is attributed to antiferromagnetic coupling between independent lattices[18] below 7 kbar.[19] Above 8 kbar the antiferromagnetic coupling between the interpenetrating lattices leads to bulk ferrimagnetic behavior.[17] This is theorized to be the result of a high-to-low-spin transition in the paddlewheel moiety.[19] Similar pressure induced spin transition phenomena have been reported previously for compounds containing transition metals.[20]

The greater steric bulk arising from the terminal *t*-Bu groups causes the bulk structure of $[Ru_2(O_2CBu^t)_4]_3[M(CN)_6]\cdot 2H_2O$ to be 2-D layers with differing terminal and intralayer connectivity between the $[Ru_2(O_2CBu^t)_4]^+$ and $[M(CN)_6]^{3-}$ ions, Figure 1, with respect to the single position for **1**.[15,21] The terminal dimer position is similar to that observed for **1** with linear Ru−N−C bonds, while the intralayer position has a significantly nonlinear Ru−N−C bond angle of 149.8°.[21] The resulting magnetic properties of $[Ru_2(O_2CBu^t)_4]_3[M(CN)_6]\cdot 2H_2O$ [M = Cr (**2**), Fe, (**3**)] are significantly enhanced from **1**, Table 1.

Herein, the pressure-dependent magnetic behavior of **2** and **3** are reported, and the results are compared to **1** and the iron analogue $[Ru_2(O_2CMe)_4]_3[Fe(CN)_6]$ (**4**).

EXPERIMENTAL SECTION

Compounds **2** and **3** were prepared by a variation to the literature method,[21,22] as $[Ru_2(O_2CBu^t)_4]Cl$ was dissolved in 5 ± 2 mL of MeOH. This solvent was selected due to its ability to readily dissolve $[Ru_2(O_2CBu^t)_4]Cl$ and its miscibility in H_2O. Infrared spectroscopy and ac susceptibility were used to confirm purity of **2** and **3**. IR spectra were measured from 400 to 4000 cm^{-1} on a Bruker Tensor 37 spectrometer (±1 cm^{-1}) as KBr pellets. A Quantum Design (QD) Physical Property Measurement System, PPMS 9 T, was used to perform ac susceptibility measurements as previously described.[23] Samples of **2** and **3** (3−15 mg) were loaded into gelatin capsules in an inert atmosphere glovebox and sealed with silicon grease prior to PPMS measurements. A QD Superconducting Quantum Interference Device (SQUID) Magnetic Property Measurement System (MPMS-5XL 5 T) (sensitivity = 10^{-8} emu or 10^{-12} emu/Oe at 1 T) was used to perform pressure-dependent measurements.[17,23] Samples of **2** and **3** (~1 mg) were loaded into a TeflonTM cell with ~1 mg of tin (Mallinckrodt, 99.9769%). The remaining volume of the Teflon cell

Received: October 2, 2012
Published: January 15, 2013

   dx.doi.org/10.1021/ic302148s | *Inorg. Chem.* 2013, 52, 1418−1423

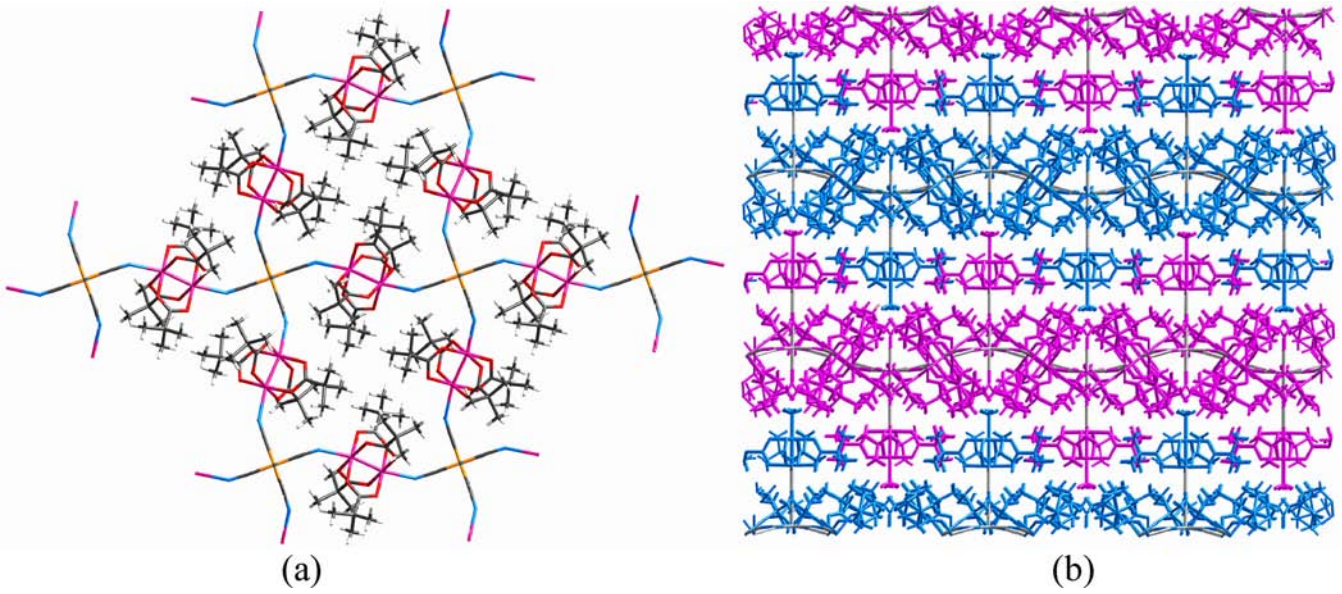

Figure 1. Layered structure of $[Ru_2(O_2CBu^t)_4]_3[M(CN)_6]\cdot 2H_2O$ [M = Cr (**2**), Fe, (**3**)]. View normal to one layer (a), and side view with adjacent layers being in different colors (b).[21]

Table 1. T_c and H_{cr} Values for 1−4

compd	M	M_s[b] (emuOe/mol)	M_r[b] (emuOe/mol)	T_c[a] (K)	H_{cr}[b] (Oe)
2	Cr	16 200	7500	37.5	20000
3	Fe	24 400	3600	4.8	190
1	Cr	20 800	3840	33.0	470
4	Fe	22 700	40	2.1	10

[a]The T_c values were reported as the peak in $\chi'(T)$ measured on a QD PPMS. [b]2 K.

was filled with decalin (the hydrostatic pressure media) and capped with Teflon plugs. The Teflon sample cell was placed in a beryllium−copper hydrostatic pressure cell based on the Kyowa Seisakusho design with zirconia pistons and rubber o-rings. Pressure was applied to the assemblage by using a Kyowa Seisakusho CR-PSC-KY05-1 apparatus with a WG-KY03-3 pressure sensor. An Aikoh Engineering model-0218B digital sensor readout was used as an approximate pressure guide during pressure application. The pressure was determined in situ by measuring the superconducting critical temperature, T_{sc}, of tin, which has been calibrated as a function of pressure.[24]

RESULTS AND DISCUSSION

Prior to studying the pressure dependence of the magnetic properties of $[Ru_2(O_2CBu^t)_4]_3[M(CN)_6]$ [M = Cr (**2**), Fe (**3**)] the ambient pressure data were redetermined and compared to the literature values. The T_c values of **2** and **3** were previously determined to be 37.5 and 4.8 K, respectively, from the peak in $\chi'(T)$.[22] Since ac measurements are not viable due to the bulk of the experimental apparatus used to maintain applied pressure on the magnetic samples, magnetization, $M(T)$, measurements were performed. The T_c was determined from the linear extrapolation of the region of most negative slope of the remnant magnetization, $M_r(T)$, and is 37.8 K for **2** and 6.1 K for **3**. Previously, irreversibility was demonstrated from the 39.5-K bifurcation temperature (T_b) of the zero-field cooled, $M_{ZFC}(T)$, and field cooled, $M_{FC}(T)$, data for **2**.[22] This is somewhat lower than 41.0 K as determined in this study. The hysteretic behavior of **2** was determined from $M(H)$ measurements at 10 K. This is at a higher temperature than previously reported, due to the inclusion of superconducting Sn as a pressure indicator (T_{sc} = 3.728 K),[24] and to facilitate comparison with previous $M(H)$ studies that utilized superconducting Pb as a pressure indicator (T_{sc} = 7.203 K[25]). The H_{cr} of **2** was previously reported to be 20 000 Oe at 2 K,[22] is significantly reduced to 13 000 Oe at 5 K,[22] and is further reduced to 6380 Oe at 10 K. This inverse trend of $H_{cr}(T)$ has been previously reported.[26] The 5 T magnetization (M_s) and remnant magnetization (M_r) from the literature were, respectively, 16 200 and 7500 emuOe/mol at 2 K and 15 800 and 7500 emuOe/mol at 5 K.[22] The M_s and M_r also follow a similar trend of decreasing magnitude at elevated temperature, dropping to 14 950 and 6590 emuOe/mol at 10 K.

The pressure-dependent magnetic properties of **2** reveal that the $M_r(T)$, $M_{ZFC}(T)$, and $M_{FC}(T)$ have an onset temperature that increases while the magnetization decreases with applied pressure, Figure 2. The T_c measured by the method discussed above increases by 32.3% to 50.0 K at 10.16 kbar, and the T_b concomitantly increases by 25.6% to 51.5 K at 10.16 kbar, Figure 3.

Increasing applied pressure reduces the magnetization M_s at 5 T, the remnant magnetization (M_r), and the coercive field, H_{cr}, while the hysteretic behavior remains consistent with the ambient pressure magnetic state, Figure 4. At 10.16 kbar the M_s decreases to 13 400 emuOe/mol, the M_r to 5120 emuOe/mol, and the H_{cr} to 2380 Oe, Figure 5. This is also consistent with the results of **3** at high pressures, vide infra. This is attributed to the interatomic separations decreasing as the interlayer separation of 2-D sheets decreases with pressure, thereby increasing the interlayer and intralayer couplings simultaneously. The $M_r(T)$, $M_{ZFC}(T)$, and $M_{FC}(T)$ exhibit some degradation through repetitive cycling of pressurization, but are nominally reversible, i.e., 6% reduction in T_b and a 9% reduction in T_c, Figures 2 and 3. The hysteretic behavior was less reversible with further reductions in M_s, M_r, and H_{cr} upon release of the applied pressure.

This structural distortion and resultant coupling has been theorized to yield a phase transition to a canted antiferro-

dx.doi.org/10.1021/ic302148s | Inorg. Chem. 2013, 52, 1418−1423

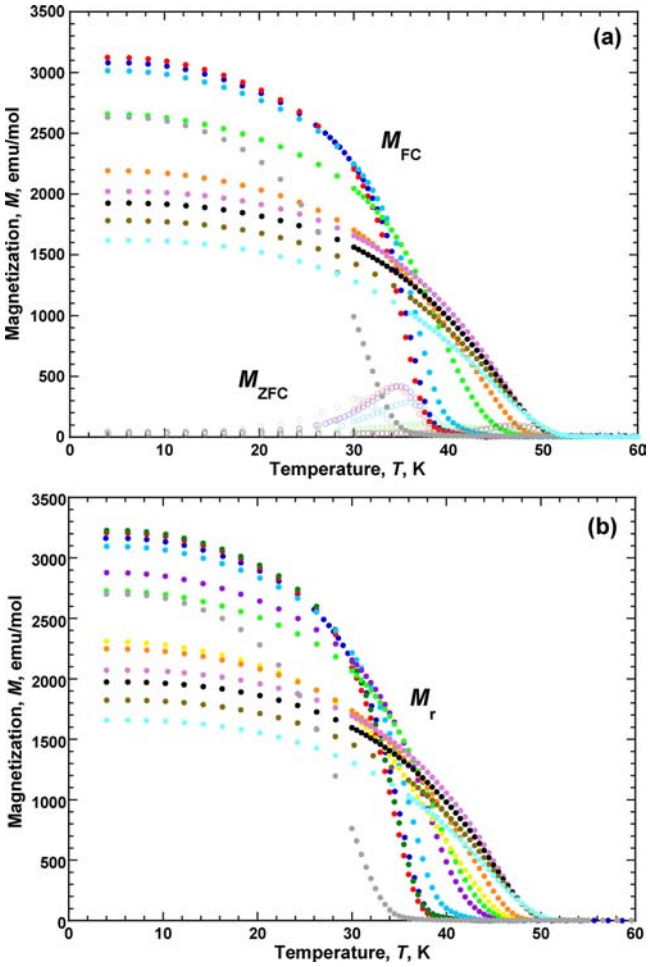

Figure 2. Pressure dependence for **2** of the M_{ZFC} and M_{FC}: 0.45 (blue ○●), 0.62 (red ○●), 1.79 (turquoise ○●), 3.58 (neon green ○●), 4.64 (orange ○●), 6.82 (pink ○●), 7.95 (black ○●), 8.58 (brown ○●), and 10.16 (light blue ○●) kbar and applied pressure released to 0.85 kbar (gray ○●) (a). For M_r: 0.45 (blue ●), 0.52 (green ●), 0.62 (red ●), 1.79 (turquoise ●), 2.73 (purple ●), 3.58 (neon green ●), 4.19 (yellow ●), 4.64 (orange ●), 6.82 (pink ●), 7.95 (black ●), 8.58 (brown ●), and 10.16 (light blue ●) kbar and applied pressure released to 0.85 kbar (gray ●) (b).

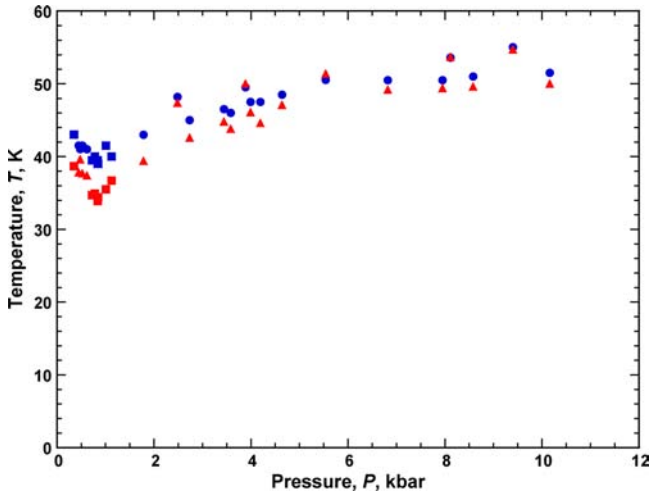

Figure 3. $T_c(P)$ (red ▲) and $T_b(P)$ (blue ●) (the released pressure measurements are shown as ■ for **2** showing a linear increase with applied pressure, and reversibility with a slight decrease after successive pressure and release cycles).

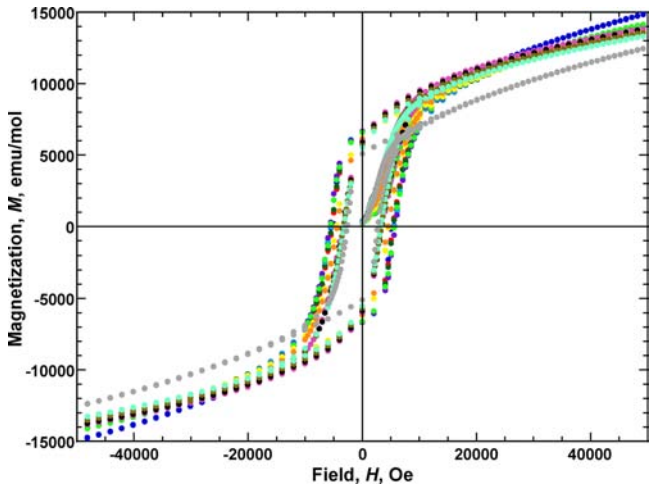

Figure 4. Field-dependent magnetization at 10 K for **2**: 0.45 (blue ●), 0.52 (green ●), 0.62 (red ●), 1.79 (turquoise ●), 2.73 (purple ●), 3.58 (neon green ●), 4.19 (yellow ●), 4.64 (orange ●), 6.82 (pink ●), 7.95 (black ●), 8.58 (brown ●), and 10.16 (light blue ●) kbar and applied pressure released to 0.85 kbar (●).

magnetic state (CAF), where the net orientation of spin on the $S = {}^3/_2$ $[Ru_2(O_2CBu^t)_4]^+$ is equal and opposite to the $S = {}^3/_2$ Cr^{III} spin.[27] Furthermore, the transition from the ambient pressure collinear ferrimagnetic phase to CAF would be evident as a "kink", or discontinuity, in the $M(T)$ data.[27] Since this is not observed, higher pressure seems to be required.

Alternatively, the decreasing intralayer bond lengths increasing the intralayer coupling would account for the observed trend of both T_b and T_c increasing with applied pressure. The simultaneously decreasing interlayer separation would increase the interlayer coupling, likely antiferromagnetic, as occurs between the sublattices in **1**.[19] Antiferromagnetic coupling between sublattices for **1** led to metamagnetic behavior and suppressed the H_{cr}.[17,19] Compounds **2** and **3** appear to have larger interlayer antiferromagnetic coupling as the pressure is increased suppressing H_{cr}, M_r, and to a lesser extent M_s. Complex pressure-dependent suppression of the H_{cr}, M_r, and M_s was observed in the 2-D layered organic-based magnet, $[Fe^{II}(TCNE)(NCMe)_2][Fe^{III}Cl_4]$, and was hypothesized to arise from increasing antiferromagnetic interlayer coupling.[28]

$[Ru_2(O_2CBu^t)_4]_3[Fe(CN)_6]$ (**3**) magnetically orders below 4.8 K with a 5 T M_s of 24 400 emuOe/mol, a M_r of 3600 emuOe/mol, and a H_{cr} of 190 Oe at 2 K and ambient pressure.[22] These properties were redetermined by measurements appropriate for pressurized studies. Similar measurement limitations arising from the inclusion of Sn as a pressure indicator occur for **3** as for **2**. The T_c from $M_r(T)$ was 6.1 K, the M_s was 22 810 emuOe/mol, the M_r was 180 emuOe/mol, and the H_{cr} was 5 Oe at 4 K at ambient pressure. These values are consistent with the corresponding decreases observed at 5 K for **2**.[26] The redetermined T_c, while significantly larger than the literature value of 4.8 K, is consistent with the value from the onset of $\chi''(T)$, ~6 K, which was not previously reported.[22]

Under increasing hydrostatic pressure, the $M_r(T)$, $M_{ZFC}(T)$, and $M_{FC}(T)$ decrease in both magnetization and onset temperature, Figure 6. The $M_{ZFC}(T)$ peak shifts to lower

dx.doi.org/10.1021/ic302148s | Inorg. Chem. 2013, 52, 1418−1423

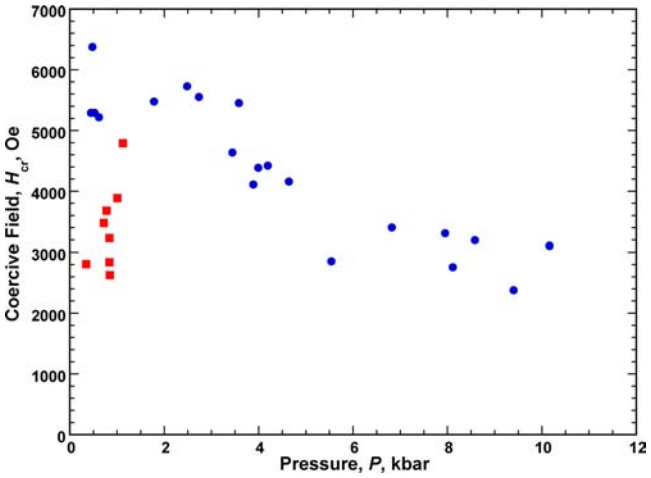

Figure 5. $H_{cr}(P)$ for **2** (blue ●) released pressure measurements (red ■). The released measurements are shown from a series of increasing pressures, with the largest H_{cr} values arising from the lowest released applied pressures. The released measurements indicate an irreversible hysteretic behavior.

temperatures as pressure was increased, and was increasingly obscured due to the lower temperature limit of measurement. The T_c determined from $M_r(T)$ increases by 13% to 6.9 K at 9.28 kbar, but displays a plateau at intermediate pressures, Figure 7. Simultaneously, the T_b increases by 55% from 5.6 to 8.7 K at 9.28 kbar, but does not display a plateau, Figure 7.

Increasing applied pressure reduces the magnetization at 5 T, while both the M_r and the H_{cr} significantly increase. The hysteresis remains consistent with the ambient pressure magnetic state even though both M_r and H_{cr} increase, Figure 8. The H_{cr} increased 11-fold to 65 Oe at 2.43 kbar, but then decreased to zero as the pressure was increased to 9.28 kbar, Figure 9. Upon release of the applied pressure to near ambient conditions the $M_r(T)$, $M_{ZFC}(T)$, $M_{FC}(T)$, and $M(H)$ display reversibility with no apparent degradation as was observed for **2**. The large relative increase in H_{cr} upon pressurization is reasonable due to the proximity in temperature of the field-dependent measurements to T_c. Quenching of the hysteretic behavior at higher applied pressures may suggest a phase transition to a metamagnetic state; however, this is inconsistent with theoretical prediction.[27] The observance of H_{cr} at intermediate pressures also does not support a phase transition. The suppression of H_{cr} above 2.43 kbar and the consistent increase of T_b with applied pressure suggests that **3** compresses similar to that proposed for **2**, resulting in simultaneous intralayer and interlayer coupling increases. However, the ratio of intra/interlayer coupling for **3** differs from **2** likely due to the evidence of reversibility in the former. Finally, the reversibility of **3** suggests a structural difference from **2** under pressure, which is not yet understood.

The pressure dependences of H_{cr}, T_c, and T_b suggest a more complex behavior than was observed for **2**. As pressure is increased below 2.4 kbar a similar structural change is expected for **2** and **3**. T_b and T_c would suggest this, while the precipitous increase in H_{cr} would at first seem contradictory. This can be explained by the proximity of the field-dependent measurements to the T_c. Proportionally the separation is quite small compared to the field-dependent measurement temperatures and T_c for **2**. Thus, a small increase in T_c or T_b through the application of pressure for **3** would result in a proportionally

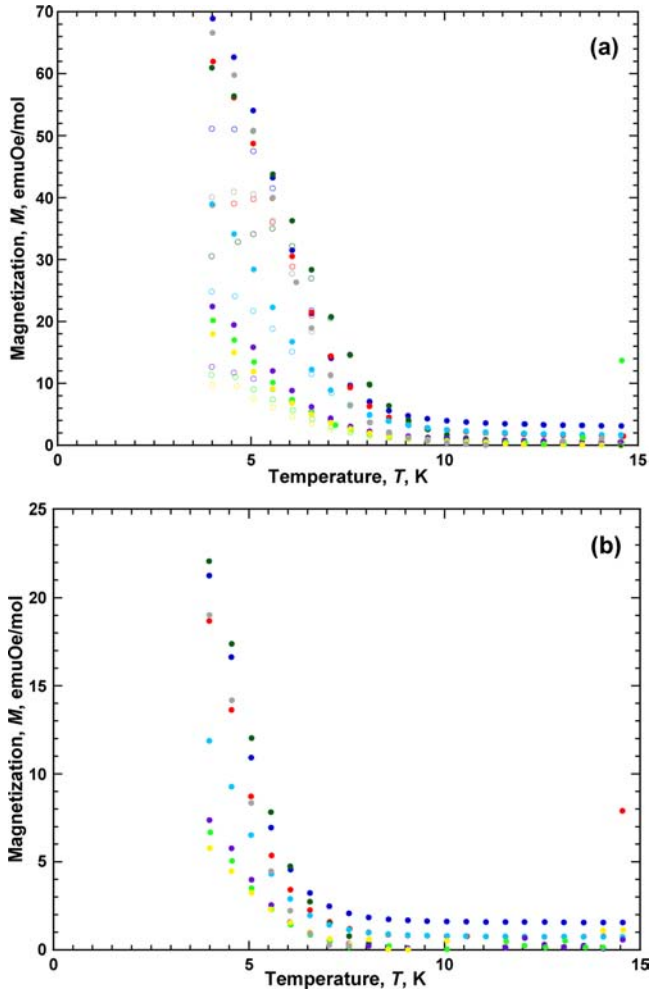

Figure 6. Pressure dependence for **3** of the M_{ZFC} and M_{FC}: 0.001 (blue ○●), 0.64 (red ○●), 2.43 (green ○●), 4.37 (turquoise ○●), 6.02 (purple ○●), 8.08 (neon green ○●), and 9.28 (yellow ○●) kbar and applied pressure released to 0.58 kbar (gray ○●) (a). For M_r: 0.001 (blue ●), 0.64 (red ●), 2.43 (green ●), 4.37 (turquoise ●), 6.02 (purple ●), 8.08 (neon green ●), and 9.28 (yellow ●) kbar and applied pressure released to 0.58 kbar (gray ●) (b).

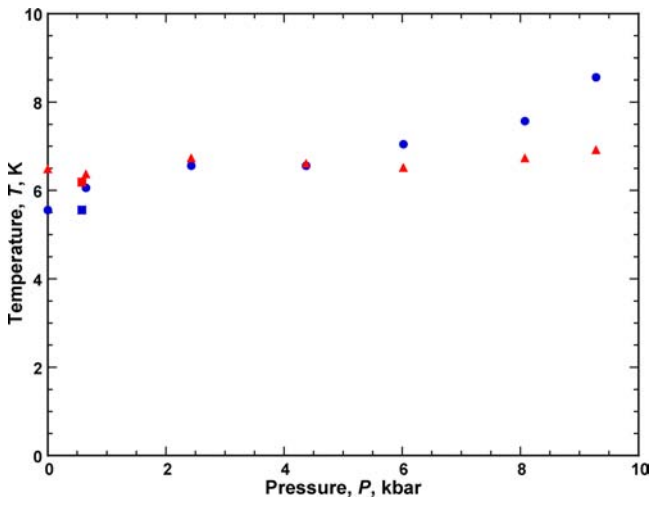

Figure 7. $T_c(P)$ (red ▲) and $T_b(P)$ (blue ●) for **3** (the released pressure measurements are shown as ■).

dx.doi.org/10.1021/ic302148s | Inorg. Chem. 2013, 52, 1418−1423

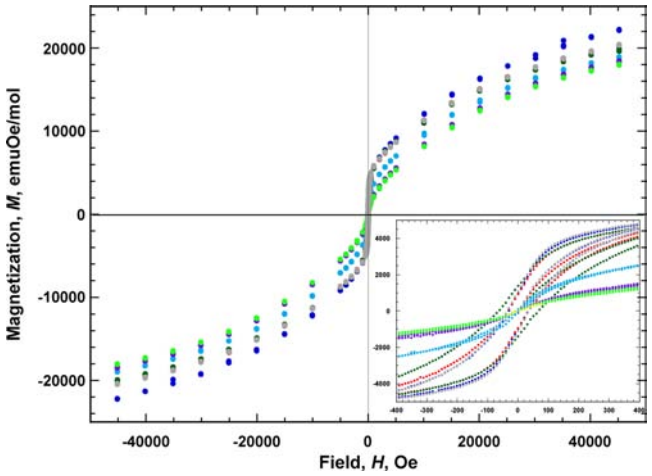

Figure 8. $M(T,P)$ at 4 K for **3**, displaying an increasing H_{cr} as pressure increased, then quenched at intermediate pressure and displayed reversibility as pressure was released: 0.001 (blue ●), 0.64 (red ●), 2.43 (green ●), 4.37 (turquoise ●), 6.02 (purple ●), 8.08 (neon green ●), and 9.28 (yellow ●) kbar and applied pressure released to 0.58 kbar (gray ●).

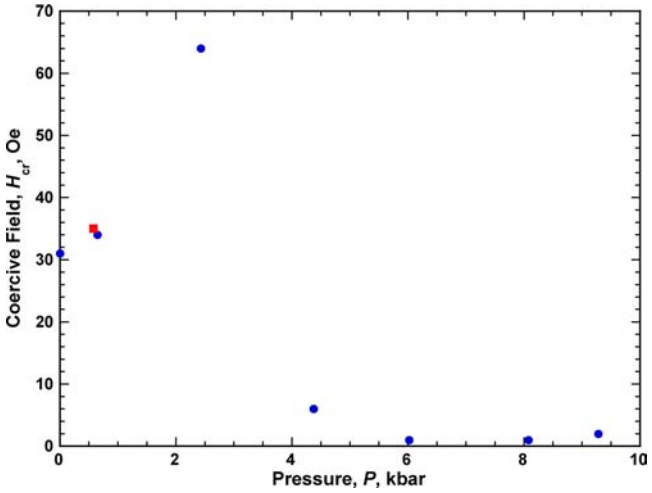

Figure 9. H_{cr} determined from field-dependent hysteretic measurements of **3** are shown (blue ●), released pressure measurement (red ■). The released measurements indicate a reversible hysteretic behavior. This is coincident with the T_b data, see text.

greater reduction in proximity of the field-dependent measurement temperature than in **2**. H_{cr} has previously been shown to rely exponentially on the proximity of the measurement temperature to T_c in metamagnets and linearly in canted systems.[15,21,26] Above 2.4 kbar the plateau in T_c and T_b and the decrease in H_{cr} suggest a few possibilities. The plateau behavior is indicative of interlayer separation reaching a minimum, which the range of pressures utilized is incapable of surpassing, similar to the behavior of $[Fe^{II}(TCNE)(NCMe)_2][Fe^{III}Cl_4]$.[28]

CONCLUSION

The layered structures **2** and **3** displayed increases in T_c and T_b with increased pressure and a propensity for the magnetic behavior to begin to quench at high pressure. Compound **3** displayed a relatively large increase in H_{cr}, before quenching to antiferromagnetic behavior above 2.43 kbar. This is in agreement with the onset of a plateau in T_b and T_c above the same pressure. The quenching exhibited by **3** is in accord with the decrease in H_{cr} of **2** as pressure was applied. Compound **2** displayed irreversibility of the hysteretic properties, H_{cr} and M_r, and to a lesser degree of the temperature-dependent properties, T_c and T_b, after the release of applied pressure. Similar complex behavior was investigated through pressure-dependent IR spectroscopy coupled with computational simulations, which focused on the CN stretching frequencies.[28] This technique could be adapted for **2** and **3** to determine the nature of bond compression, bending, or deformation upon application of pressure. The computational simulation was previously used to support the hypothesis that pressure application induced stronger interlayer antiferromagnetic coupling and to explain the red or blue shift of the CN stretching frequency as either compression or bending.[28] Hypotheses in the absence of pressure-dependent structural clues are necessarily limited.

AUTHOR INFORMATION

Corresponding Author

*E-mail: jsmiller@chem.utah.edu.

Notes

The authors declare no competing financial interest.

ACKNOWLEDGMENTS

We appreciate Royce A. Davidson for his assistance with diamagnetic corrections due to the excessive mass of the BeCu pressure apparatus, and the continued support by the U.S. National Science Foundation (DMR-11063630).

REFERENCES

(1) Benecki, W.; Clagett, T.; Trout, S. *Permanent Magnets 2010–2020— A Comprehensive Overview of the Global Permanent Magnet Industry*; Report No. 9-21, 55, 2010.
(2) Miller, J. S. *Chem. Soc. Rev.* **2011**, *40*, 3266.
(3) Blundell, S. J.; Pratt, F. L. *J. Phys.: Condens. Matter* **2004**, *16*, R771.
(4) Ovcharenko, V. I.; Sagdeev, R. Z. *Russ. Chem. Rev.* **1999**, *68*, 345.
(5) Miller, J. S.; Epstein, A. J. *Angew. Chem., Int. Ed. Engl.* **1994**, *33*, 385.
(6) Miller, J. S.; Calabrese, J. C.; Rommelmann, H.; Chittipeddi, S. R.; Zhang, J. H.; Reiff, W. M.; Epstein, A. J. *J. Am. Chem. Soc.* **1987**, *109*, 769.
(7) Miller, J. S. *J. Mater. Chem.* **2010**, *20*, 1846.
(8) Varret, F.; Nogues, M.; Goujon, A. In *Magnetism: Molecules to Materials*; Miller, J. S., Drillon, M., Eds.; Wiley-VCH: New York, 2000, Vol. *1*, p 257.
(9) Bozdag, K. D.; Yoo, J.-W.; Raju, N. P.; McConnell, A. C.; Miller, J. S.; Epstein, A. J. *Phys. Rev. B* **2010**, *82*, 094449.
(10) Manriquez, J. M.; Yee, G. T.; McLean, R. S.; Epstein, A. J.; Miller, J. S. *Science* **1991**, *252*, 1415.
(11) Miller, J. S. *Polyhedron* **2009**, *28*, 1596.
(12) (a) Ferlay, S.; Mallah, T.; Ouahes, R.; Veillet, P.; Verdaguer, M. *Nature* **1995**, *378*, 701. (b) Dujardin, E.; Ferlay, S.; Phan, X.; Desplanches, C.; Moulin, C. C. D.; Sainctavit, P.; Baudelet, F.; Dartyge, E.; Veillet, P.; Verdaguer, M. *J. Am. Chem. Soc.* **1998**, *120*, 11347. (c) Ferlay, S.; Mallah, T.; Ouahes, R.; Veillet, P.; Verdaguer, M. *Inorg. Chem.* **1999**, *38*, 229. (d) Verdaguer, M.; Bleuzen, A.; Train, C.; Garde, R.; Fabrizi de Biani, F.; Desplanches, C. *Phil. Trans. R. Soc., A* **1999**, *357*, 2959.
(13) Holmes, S. M.; Girolami, G. S. *J. Am. Chem. Soc.* **1999**, *121*, 5593.
(14) Hatlevik, Ø.; Buschmann, W. E.; Zhang, J.; Manson, J. L.; Miller, J. S. *Adv. Mater.* **1999**, *11*, 914.
(15) Liao, Y.; Shum, W. S.; Miller, J. S. *J. Am. Chem. Soc.* **2002**, *124*, 9336.

(16) Vos, T. E.; Liao, Y.; Shum, W. W.; Her, J.-H.; Stephens, P. W.; Reiff, W. M.; Miller, J. S. *J. Am. Chem. Soc.* **2004**, *126*, 11630.
(17) Shum, W. S.; Her, J.-H.; Stephens, W.; Lee, Y.; Miller, J. S. *Adv. Mater.* **2007**, *19*, 2910.
(18) Shum, W. W.; Liao, Y.; Miller, J. S. *J. Phys. Chem. A* **2004**, *108*, 7460.
(19) Fishman, R. S.; Shum, W. W.; Miller, J. S. *Phys. Rev. B* **2010**, *81*, 172407.
(20) (a) Takano, M.; Nasu, S.; Abe, T.; Yamamoto, K.; Endo, S.; Takeda, Y.; Goodenough, J. B. *Phys. Rev. Lett.* **1991**, *67*, 3267. (b) Rueff, J.-P.; Kao, C.-C.; Struzhkin, V. V.; Badro, J.; Shu, J.; Hemley, R. J.; Mao, H. K. *Phys. Rev. Lett.* **1999**, *82*, 3284. (c) Aguado, F.; Rodriquez, F.; Núñez, P. *Phys. Rev. B* **2007**, *76*, 094417. (d) Golosova, N. O.; Kozlenko, D. P.; Dubrovinsky, L. S.; Drozhzhin, O. A.; Istomin, S. Y.; Savenko, B. N. *Phys. Rev. B* **2009**, *79*, 104431.
(21) Yoshioka, D.; Mikuriya, M.; Handa, M. *Chem. Lett.* **2002**, 1044.
(22) Vos, T. E.; Miller, J. S. *Angew. Chem., Int. Ed.* **2005**, *44*, 2416.
(23) Kareis, C. M.; Her, J.-H.; Stephens, P. W.; Moore, J. G.; Miller, J. S. *Chem.—Eur. J.* **2012**, *18*, 9281. Brandon, E. J.; Rittenberg, D. K.; Arif, A. M.; Miller, J. S. *Inorg. Chem.* **1998**, *37*, 3376.
(24) Jennings, L. D.; Swenson, C. A *Phys. Rev.* **1958**, *112*, 31.
(25) Clark, M. J.; Smith, T. F. *J. Low Temp. Phys.* **1978**, *32*, 495.
(26) Rittenberg, D. K.; Sugiura, K.-I.; Sakata, Y.; Mikami, S.; Epstein, A. J.; Miller, J. S. *Adv. Mater.* **2000**, *12*, 126.
(27) Fishman, R. S.; Okamoto, S.; Miller, J. S. *Phys. Rev. B* **2009**, *80*, 140416.
(28) Shum, W. W.; Lee, Y.; Stephens, P. W.; Liu, Z.; Miller, J. S. Unpublished results.

dx.doi.org/10.1021/ic302148s | *Inorg. Chem.* 2013, 52, 1418−1423